PORTLAND PRESS

BIOCHEMICAL JOURNAL
ACCEPTED MANUSCRIPT

Psoriasis mutations disrupt CARD14 autoinhibition promoting BCL10-MALT1-dependent NF-κB activation

Ashleigh Howes, Paul A. O'Sullivan, Felix Breyer, Ashavari Ghose, Li Cao, Daniel Krappmann, Anne M. Bowcock & Steven C. Ley

Inherited and *de novo* mutations in the *CARD14* gene promote the development of psoriasis, an inflammatory disease of the skin. CARD14 is a member of the CARMA protein family that includes the structurally related CARD11 adaptor that mediates NF-κB activation by antigen receptors. We investigated the mechanism by which *CARD14* mutation in psoriasis activates NF-κB. In contrast to wild type CARD14, $CARD14^{E138A}$ and $CARD14^{G117S}$ psoriasis mutants interacted constitutively with BCL10 and MALT1, and triggered BCL10 and MALT1 dependent activation of NF-κB in keratinocytes. These alterations disrupted the inhibitory effect of the CARD14 linker region on NF-κB activation by facilitating BCL10 binding. Therefore, psoriasis mutations activated CARD14 by a mechanism analogous to oncogenic CARD11 mutations in non-Hodgkin B cell lymphomas. $CARD14^{E138A}$ also stimulated MALT1 paracaspase activity and activated both ERK1/2 and p38α MAP kinases. Inhibition of MALT1 with mepazine reduced $CARD14^{E138A}$-induced expression of specific psoriasis-associated transcripts in keratinocytes. Our results establish the mechanism whereby gain-of-function CARD14 variants, which induce psoriatic disease in affected individuals, activate pro-inflammatory signaling.

Cite as Biochemical Journal (2016) DOI: 10.1042/BCJ20160270

Psoriasis mutations disrupt CARD14 autoinhibition promoting BCL10-MALT1-dependent NF-κB activation

Ashleigh Howes[1,2], Paul A. O'Sullivan[2], Felix Breyer[2], Ashavari Ghose[2,], Li Cao[3], Daniel Krappmann[4], Anne M. Bowcock[1]* & Steven C. Ley[2]*

[1]National Heart and Lung Institute, Imperial College London, London, UK
[2]The Francis Crick Institute - Mill Hill Laboratory, London, UK
[3]Dept. of Genetics, Washington University in Saint Louis, MO, USA
[4] Research Unit Cellular Signal Integration, Institute of Molecular Toxicology and Pharmacology, Helmholtz Zentrum München - German Research Center for Environmental Health, Neuherberg, Germany.

Short title: CARD14 activation of NF-κB in psoriasis

Key words: CARD14 / keratinocytes / MALT1 / NF-κB / psoriasis

* **Corresponding authors**:
Anne Bowcock
Email: a.bowcock@imperial.ac.uk
Steven Ley
Email: steve.ley@crick.ac.uk

ABSTRACT

Inherited and *de novo* mutations in the *CARD14* gene promote the development of psoriasis, an inflammatory disease of the skin. CARD14 is a member of the CARMA protein family that includes the structurally related CARD11 adaptor that mediates NF-κB activation by antigen receptors. We investigated the mechanism by which *CARD14* mutation in psoriasis activates NF-κB. In contrast to wild type CARD14, CARD14^{E138A} and CARD14^{G117S} psoriasis mutants interacted constitutively with BCL10 and MALT1, and triggered BCL10 and MALT1 dependent activation of NF-κB in keratinocytes. These alterations disrupted the inhibitory effect of the CARD14 linker region on NF-κB activation by facilitating BCL10 binding. Therefore, psoriasis mutations activated CARD14 by a mechanism analogous to oncogenic CARD11 mutations in non-Hodgkin B cell lymphomas. CARD14^{E138A} also stimulated MALT1 paracaspase activity and activated both ERK1/2 and p38α MAP kinases. Inhibition of MALT1 with mepazine reduced CARD14^{E138A}-induced expression of specific psoriasis-associated transcripts in keratinocytes. Our results establish the mechanism whereby gain-of-function CARD14 variants, which induce psoriatic disease in affected individuals, activate pro-inflammatory signaling.

SUMMARY STATEMENT

We have found that psoriasis-associated *CARD14* mutations release the CARD14 protein from autoinhibition, inducing constitutive formation of CARD14-containing signaling complexes. These activate NF-κB and MAP kinase signaling pathways, which drive the pathogenic expression of pro-inflammatory genes in skin cells.

ABBREVIATIONS

CARD14; caspase recruitment domain-containing protein 14
CARMA; CARD-containing MAGUK protein
coIP; co-immunoprecipitation
ERK1/2; extracellular signal-regulated kinase 1/2
IKK2; inhibitor of NF-κB (IκB) kinase 2
MAGUK; membrane-associated guanylate kinase
MAP kinase; mitogen-activated protein kinase
TR; tetracycline (Tet) repressor

INTRODUCTION

Psoriasis is a chronic inflammatory skin disease that arises through interactions between hyper-proliferative keratinocytes and activated immune cells that infiltrate the skin (1). The disease affects 2-4% of USA and European adults, of which 20-30% also develop psoriatic arthritis (PsA). Genome-wide association studies (GWAS) have identified multiple genetic loci that individually confer low risk for the development of psoriasis (2). Many of these genes highlight the importance of immune system in disease development, encoding proteins involved in antigen presentation, T cell polarization and innate immunity. However, identified genetic loci explain less than 20% of disease variance suggesting that rare variants may contribute to the remaining portion, in addition to further unknown low risk loci and genetic interactions.

We have discovered highly penetrant *de novo* and inherited, dominant gain-of-function mutations in the *CARD14* gene that promote the development of psoriasis and PsA (3, 4). Among these, the *de novo* CARD14^{E138A} mutation was identified in a child with early-onset generalized pustular psoriasis and is considered severe. The CARD14^{G117S} mutation, which leads to point mutation and altered splicing of the *CARD14* transcript, was identified in a family of European descent and a Tunisian cohort with multiple cases of psoriasis and PsA (4, 5). A second multiply affected family from Taiwan harboured a mutation in the exon 3 splice donor site that affected splicing in a similar manner to the CARD14^{G117S} mutation (4, 5). Although these pathogenic variants are rare, the common CARD14 polymorphism (R820W) exceeds genome-wide significance for association with psoriasis and PsA (6-8). These findings indicate that CARD14 variants may have a more widespread role in the pathogenesis of psoriasis and PsA and are not restricted to rare families with highly penetrant mutations.

CARD14 (CARMA2) is a member of the CARMA family of scaffolding proteins (9). This includes CARD11 and CARD10, which play critical roles in the activation of NF-κB transcription factors in response to ligation of antigen receptors and G-protein-coupled receptors, respectively. NF-κB transcription factors, composed of dimers of Rel polypeptides, regulate gene expression by binding to κB elements in the promoters and enhancers of multiple target genes that regulate immune and inflammatory responses (10). CARD14 (CARMA2) has a similar domain structure to CARD11 (CARMA1) and CARD10 (CARMA3) (Figure 1A), comprising an N-terminal CARD domain, followed by a coiled-coil (CC) domain, and a C-

terminal MAGUK domain (PDZ-SH3-GUK), and activates NF-κB when overexpressed in HEK293 cells (11). A shorter isoform CARD14sh (12) is expressed most highly in the skin (4). CARD14sh lacks the C-terminal MAGUK domain of CARD14, similar to the related protein CARD9 that mediates activation of NF-κB by the C-type lectin receptor dectin-1 (9).

The structural similarity to CARD11, CARD10 and CARD9 suggests a role for CARD14 in NF-κB activation. Consistent with this, wild type (WT) CARD14 overexpression activates an NF-κB reporter in HEK293 cells (11). Furthermore, we have shown that transfected CARD14 stimulates NF-κB in keratinocytes and endothelial cells, and that this activity is amplified when CARD14 harbors psoriasis-associated mutations (3, 4). CARD14 overexpression additionally induces the expression of a subset of psoriasis-associated genes in keratinocytes. NF-κB is constitutively active in psoriatic skin, and GWAS have identified genetic alterations in components of the NF-κB pathway in psoriasis and PsA (13). Thus, CARD14 likely plays an important role in psoriasis pathogenesis through its ability to trigger NF-κB-dependent-inflammation within the skin. Consistent with this model, we have found that CARD14 is highly expressed in keratinocytes of the basal and supra-basal skin epithelial layers (4). CARD14 is additionally expressed in dermal, lymphatic and aortic endothelial cells (14), suggesting that CARD14 mutations may contribute to cardiovascular and other systemic comorbidities associated with psoriasis.

The mechanism by which the related family member CARD11 activates canonical NF-κB in T cells has been studied in detail (9). Following T cell receptor (TCR) stimulation, CARD11 is activated by recruitment to the plasma membrane via its MAGUK domain, and phosphorylation of its linker region by protein kinase C (PKC) θ. This induces a conformational change that allows CARD11 to recruit the preformed complex of BCL10 (B cell lymphoma protein 10) and MALT1 (Mucosa-associated lymphoid tissue lymphoma translocation protein 1), a paracaspase (15). TCR-induced formation of the CARD11-BCL10-MALT1 (CBM) complex is critical for TCR activation of NF-κB transcription factors. Similarly, the CBM complex is essential for B cell receptor (BCR) activation of NF-κB. BCL10 and MALT1 are also required for CARD10 activation of NF-κB by G protein-coupled receptors (GPCRs) in fibroblasts, indicating that a CARD10-BCL10-MALT1 complex may play an analogous role to the CARD11-BCL10-MALT1 complex in antigen-stimulated lymphocytes.

In this study, we investigated the mechanism by which highly penetrant psoriasis-inducing CARD14 mutations stimulate NF-κB. We show that E138A and G117S psoriasis mutations promoted CARD14 interaction with BCL10 and MALT1, and that mutant CARD14 activation of NF-κB in keratinocytes was dependent on expression of both of these proteins. Mutations were found to activate constitutive CARD14 signaling by disrupting the inhibitory effect of the linker domain located between the coiled-coil and PDZ domains. CARD14 psoriasis variants also stimulated MALT1 paracaspase activity, and experiments with the MALT1 inhibitor mepazine demonstrated that this was required for maximal CARD14 activation of NF-κB and induced expression of specific pro-inflammatory cytokine and chemokine gene transcripts.

EXPERIMENTAL

Expression constructs

Human CARD14fl cDNA was purchased from TrueORF (RC217455), human CARD14sh cDNA was purchased from Capital Biosciences (DHC-3073-M11). E138A (c.413A>C) and G117S (c.349G>A also causing 66 bp insertion of intronic sequence after exon 3) mutations were introduced as previously described (4) . All CARD14 inserts were cloned into pcDNA3 (Invitrogen) with either a C-terminal V5 (GKPIPNPLLGLDST) or 3xFLAG (DYKDHDGDYKDHDIDYKDDDDK) tag (Sigma). Linker region deleted (ΔLR) CARD14 constructs were generated by deletion of c.1228-1722 using overlap extension PCR. Deletion of this sequence was determined by CARD14 domain boundary prediction (JPred and Uniprot). Human MALT1 (isoform A) cDNA was purchased from GeneCopoeia (EX-T0622-M11) and cloned into pcDNA3 with an N-terminal 3xFLAG tag. C464A mutation (c.1471-1473, TGT>GCT) was introduced into MALT1 by site directed mutagenesis. Human BCL10 cDNA was cloned into pcDNA3 with an N-terminal HA (YPYDVPDYA) or 3xFLAG tag.

Reagents

Antibodies used in this study were: anti-V5 (Serotec MCA1360); anti-FLAG M2 (Sigma F3165); anti-HA (Roche 11867423001); anti-BCL10 (sc-56); anti-MALT1 (sc-46677); anti-TUBULIN (TAT-1); p105 (CST 4717); phospho-p105 (CST 4806); ERK1/2 (sc-93, sc-154); phospho-ERK1/2 (CST 9101); p38 (CST 9212); phospho-p38 (CST 4511); phospho-JNK (Invitrogen 44682); JNK (CST 9252). Mepazine was purchased from Calbiochem, PD0325901 and VX-745 were from Selleck Chemicals, BI605906 was obtained through the MRC PPU Reagents and Services facility (MRC PPU, College of Life Sciences, University of Dundee, Scotland, mrcppureagents.dundee.ac.uk).

Immunoprecipitations

$1x10^6$ HEK293 cells were seeded in 90 mm dishes (10 ml per dish) in DMEM, 10% FCS, 2 mM L-glutamine, 100 U penicillin, 0.1 mg/ml streptomycin. The next day cells were transfected using Lipofectamine (Invitrogen) following the manufacturer's instructions. cDNA amounts of various constructs are indicated in corresponding figure legends. After 24 h cells were lysed in 1 ml coIP buffer (50 mM Tris pH 7.5, 150 mM NaCl, 1% Triton-X, 10% glycerol, 2 mM EDTA , 10 mM sodium flouride, 1 mM sodium pyrophosphate, 10 mM β-glycerophosphate, 0.1 mM sodium vanadate, 10 mM iodoacetamide and protease inhibitor cocktail

[Roche 11836170001]). Lysates were centrifuged at 14,000 rpm for 10 min to clear debris. Protein levels were quantified (Pierce BCA protein assay, Thermo Scientific) and normalised. Lysates were precleared with IgG Agarose (Sigma) for 1 h rotating, 4°C. 55 µl of precleared lysate was saved for analysis by western blotting. Remaining precleared lysate was incubated with a 10 µl bead volume of anti-FLAG M2 affinity gel (Sigma) overnight with rotation, 4°C. Beads were subsequently washed (5 min rotating, 4°C) twice with high salt buffer (50 mM Tris pH 7.5, 500 mM NaCl, 1% Triton-X, 10% glycerol, 2 mM EDTA , 10 mM sodium flouride, 1 mM sodium pyrophosphate, 10 mM β-glycerophosphate, 0.1 mM sodium vanadate, 10 mM iodoacetamide) and four times with coIP buffer. Beads were dried and eluted three times by incubation with 10-15 µl glycine buffer (0.2 M glycine, 0.05% NP-40, pH 2.5) for 3 min at RT with agitation. Pooled eluates were neutralised with Tris pH 8, boiled for 5 min with Laemmli buffer and resolved by SDS-PAGE for analysis.

NF-κB Luciferase assays

$1x10^5$ HaCaT keratinocytes were seeded in 24 well plates (500 µl per well) in DMEM, 10% FCS, 2 mM L-glutamine, 100 U penicillin, 0.1 mg/ml streptomycin overnight. Cells were then co-transfected with 3xFLAG-CARD14 cDNA, pNF-κB-Luc reporter (0.25 µg, Clontech 631904) and pRL-TK control reporter (0.05 µg, Promega E2241) using Lipofectamine 2000 (Invitrogen) following the manufacturer's instructions. CARD14 cDNA amounts per transfection are indicated in corresponding figure legends and total cDNA was normalised across experiments with pcDNA3 empty vector (EV). 24 h after transfection cells were lysed in 60 µl Passive Lysis Buffer (Promega) and analysed using the Dual Luciferase Reporter Assay System (Promega) according to the manufacturer's instructions. Relative NF-κB activation was determined by normalising pNF-κB-Luc reporter activity to pRL-TK activity, and then dividing all values to activity induced by EV alone. CARD14 expression levels in corresponding total cell lysates were determined by western blotting. BCL10 and MALT1 knockdown efficiency was calculated by densitometric quantification of immunoblots (GS800 Calibrated Densitometer, Quantity One software). Relative BCL10 and MALT1 expression was normalized to loading control values (tubulin), and then scaled according to expression with control siRNA. Average knockdown was calculated within each experiment, and then averaged across three independent experiments.

siRNA knockdown

HaCaT keratinocytes were seeded in 24 well plates at $3.75x10^4$ cells per well overnight. The following day cells were transfected with 50 µM ON-TARGET plus siRNA SMARTpools targeting *Bcl10* (sequences: GCCACCAGAUCUACAGUUA; CGAACAACCUCUCCAGAUC; GGGCAUCCACUGUCAUGUA; AAUCAUAGCUGAGAGACAU), *Malt1* (sequences: GGGAGUAUAUGGGUUAUUA; GCAGUGUUCUCUUAAGGUA; GCAAAUCUGUGUUGAACCA; GGUAAUCCAAGUAAUGUUA) or non-targeting control pool (sequences: UGGUUUACAUGUCGACUAA; UGGUUUACAUGUUGUGUGA; UGGUUUACAUGUUUUCUGA; UGGUUUACAUGUUUUCCUA) using Lipofectamine 2000 following the manufacturer's instructions. 48 h later, cells were transfected for NF-κB Luciferase assays as described above.

Malt1 activity assay

HEK293 cells were transfected for 24 h as described above. Cells were lysed in 600 µl MALT1 coIP buffer (25 mM HEPES pH 7.5, 150 mM NaCl, 0.2% NP-40, 10% glycerol, 1 mM dithiothreitol, 10 mM sodium fluoride, 8 mM β-glycerophosphate, and 300 µM sodium vanadate) without protease inhibitors. Lysates were centrifuged at 14,000 rpm for 10 min to remove debris. Protein levels were quantified and normalised. Lysates were precleared with streptavidin agarose resin (Thermo Scientific) for 1h, 4°C with rotation. 40 µl precleared lysate was saved for analysis by western blotting. Remaining lysate was incubated with 0.1 µM biotinylated ABP probe 7 (16) for 50 min, RT with rotation. 12 µl bead volume of streptavidin agarose resin was added for 2 h, 4°C with rotation. Beads were washed four times with MALT1 coIP buffer. Protein was eluted by boiling beads for 5 min in Laemmli buffer and resolved by SDS-PAGE for analysis.

Generation and protein analysis of tetracycline inducible HaCaT CARD14^{E138A} keratinocytes

3xFLAG tagged CARD14 cDNA was cloned into the pcDNA5/TO vector (Invitrogen) and transfected into HaCaT-TR cells (a kind gift from Caroline Hill; (17)), which stably express the tetracycline repressor (pcDNA6/TR, Invitrogen). Cells were expanded for 4-6 weeks in DMEM, 10% tetracycline free (TF) FCS, 2 mM L-glutamine, 100 U penicillin, 0.1 mg/ml streptomycin, 10 µg/ml blasticidin (for pcDNA6/TR maintenance) and 500 µg/ml hygromycin (for CARD14-pcDNA5/TO selection). For protein analysis, cells were seeded in 24 well plates at $1x10^5$ cells per well in DMEM, 0.1% TF FCS, 2 mM L-glutamine, 100 U penicillin, 0.1 mg/ml

streptomycin overnight. Cells were then incubated in DMEM for 5 h to minimise basal signalling levels prior to the addition of 1 µg/ml tetracycline (Sigma). At the indicated times cells were lysed in 60 µl radioimmunoprecipitation assay (RIPA) buffer (50 mM Tris HCl pH 7.5, 150 mM NaCl, 2 mM EDTA, 1 mM sodium pyrophosphate, 50 mM sodium fluoride, 1 mM sodium vanadate, 0.1% SDS, 1% Triton-X, 0.5% deoxycholate and protease inhibitor cocktail). Total cell lysates were boiled in Laemmli buffer and resolved by SDS-PAGE for analysis.

Quantitative PCR

HaCaT CARD14^{E138A} cells were seeded in 24 well plates at 1x10^5 cells per well in DMEM, 1% TF FCS, 2 mM L-glutamine, 100 U penicillin, 0.1 mg/ml streptomycin overnight. Cells were then incubated in DMEM in the presence of DMSO or indicated pharmacological inhibitor for 1 h prior to the addition of 1 µg/ml tetracycline. Cells were lysed 6 h later in 350 µl RLT buffer (QIAGEN), 1% β-mercaptoethanol. RNA was purified using RNAeasy mini kit (QIAGEN) according to the manufacturer's instructions. SuperScript VILO cDNA synthesis kit (Thermo Fisher) was used to transcribe cDNA according to the manufacturer's instructions. Quantitative real-time PCR was carried out using the TaqMan Assay system (Applied Biosystems). Primer probes used were: *IL8* (Hs00174103_m1); *CCL20* (Hs00355476_m1); *IL36γ* (Hs00219742_m1). Expression levels were normalised to the housekeeping gene *18S* (Hs99999901_s1) and calculated using the $2^{(-\Delta\Delta CT)}$ method.

Statistical analysis

Students t-test (two-tailed, unpaired) and two-way ANOVA (with Bonferroni multiple testing correction) analyses were conducted using GraphPad Prism version 6.00 for Mac OS X, GraphPad Software, La Jolla California USA, www.graphpad.com.

RESULTS

CARD14 activation of NF-κB requires BCL10 and MALT1

Secondary structure similarity with CARD11 and CARD10 suggested that CARD14 would form a complex with BCL10 and MALT1 to activate NF-κB (Figure 1A). To investigate this, full length (fl) and short (sh) forms of V5-CARD14 were expressed together with FLAG-MALT1 and HA-BCL10 in HEK293 cells. Wild type (WT) CARD11 does not interact with BCL10 / MALT1 to form active signaling complexes unless cells are stimulated via specific upstream receptors, such as the TCR (18). In line with this, immunoblotting revealed little detectable co-immunoprecipitation of wild type (WT) V5-CARD14fl or V5-CARD14sh with FLAG-MALT1/HA-BCL10 (Figure 1B). However, introduction of the E138A psoriasis-associated CARD14 mutation (Figure 1A) induced clear association of FLAG-MALT1/HA-BCL10 with both V5-CARD14fl and V5-CARD14sh (Figure 1B). Similarly, the V5-CARD14sh^{G117S} psoriasis variant co-purified with FLAG-MALT1/HA-BCL10 complexes (Figure 1C). Therefore, a common effect of two psoriasis-associated CARD14 mutations was formation of a CARD14-BCL10-MALT1 complex, without the need for upstream agonist stimulation.

We next tested the effect of the CARD14 psoriasis mutations on activation of an NF-κB reporter in HaCaT keratinocytes, a cell type that plays an important role in psoriasis etiology and expresses CARD14 (1, 4). Both FLAG-CARD14fl^{E138A} and FLAG-CARD14sh^{E138A} activated NF-κB, while WT FLAG-CARD14 had only a modest or no stimulatory effect (Figure 1D). FLAG-CARD14sh^{G117S} also strongly activated the NF-κB reporter (Figure 1E). SiRNA knockdown of endogenous BCL10 (77.63% knockdown ±2.3 [SEM, n=3]), significantly reduced activation of an NF-κB reporter by each of the CARD14 psoriasis variants (Figure 1 F and G). Similarly, MALT1 knockdown (70.70% knockdown ±1.90 [SEM, n=3]) significantly decreased NF-κB reporter activation by FLAG-CARD14fl^{E138A}, FLAG-CARD14sh^{E138A} and FLAG-CARD14sh^{G117S}. Together the results in this section suggested that formation of a complex with BCL10 and MALT1 was required for activation of NF-κB by CARD14 alterations seen in psoriasis.

E138A and G117S psoriasis mutations disrupt CARD14 autoinhibition

In the basal state, CARD11 signaling activity is held in check by an inhibitory domain (ID), located between the coiled-coil and PDZ domains, that interacts with the CARD and coiled-coil domains (19). CARD11 autoinhibition is relieved following antigen receptor stimulation by the inducible phosphorylation of the ID

by protein kinase C (PKC) isoforms, which triggers formation of a CARD11-BCL10-MALT1 complex (20). Oncogenic mutations in CARD11 in several types of lymphoma also interrupt ID-mediated inhibition (21). These mutations are located within the CARD11 coiled-coil domain and disrupt ID intramolecular interactions, bypassing the requirement for antigen-receptor induced ID phosphorylation for CARD11 activation of NF-κB.

Psoriasis-associated activating mutations in CARD14 are located predominantly within or adjacent to the coiled-coil domain (3, 4). The comparable secondary structure of CARD14 suggested a similar activating mechanism to oncogenic CARD11 mutations. Initially, the effect of removing the linker region (LR) between the coiled-coil and PDZ domains of WT FLAG-CARD14 was tested. Analogous to CARD11 (19), this promoted FLAG-CARD14 stimulation of NF-κB in HaCaT keratinocytes (Figure 2 A). However, LR deletion in FLAG-CARD14fl^{E138A} and FLAG-CARD14sh^{E138A} psoriasis variants did not alter their ability to activate NF-κB. Similarly, LR deletion did not alter NF-κB activation by FLAG-CARD14sh^{G117S} (Figure 2B). Consistently, the stimulatory effects of the E138A and G117S mutations on NF-κB activation were significantly reduced in the absence of the LR (Figure 2C). These results support the hypothesis that psoriasis mutations interfere with autoinhibitory function of the LR.

Deletion of the inhibitory linker domain induces binding of CARD11 to BCL10 and co-recruitment of MALT1 to promote the formation of CARD11-BCL10-MALT1 complex (19). To determine whether the linker domain of CARD14 functioned in a similar way, HEK293 cells were co-transfected with expression constructs encoding WT or LR-deleted V5-CARD14 and FLAG-BCL10. Immunoblotting of anti-FLAG immunoprecipitates revealed that FLAG-BCL10 co-purified with V5-CARD14sh/flΔLR but not V5-CARD14 (Figure 2D). V5-CARD14sh/fl^{E138A} also co-immunoprecipitated with FLAG-BCL10, but this was not further increased by LR deletion. Similarly, V5-CARD14sh^{G117S} interacted with BCL10 and this was not increased by deletion of the LR (Figure 2D). Together these results suggested that E138A and G117S psoriasis mutations abrogated LR inhibition, which facilitated BCL10 binding and NF-κB activation.

CARD14^{E138A} activates MALT1 paracaspase activity

In addition to functioning as a scaffolding protein, MALT1 is a paracaspase that cleaves substrates after arginine residues (15). MALT1 proteolytic activity is induced following T cell antigen receptor stimulation. This promotes the cleavage

of a limited number of proteins, including A20, CYLD and RelB that negatively regulate NF-κB activation. MALT1 is also activated in diffuse large B cell lymphomas that rely on chronic B cell receptor signaling (22), and MALT1 paracaspase activity promotes lymphoma survival by inactivating negative regulators of NF-κB (23). Furthermore, expression of oncogenic CARD11 is sufficient to trigger MALT1 activation in BJAB cells (16).

In this and the following sections, we focused on the E138A psoriasis CARD14 mutation, which is the most pathogenic variant (3, 4). To determine whether CARD14 could activate MALT1 paracaspase activity, HEK293 cells were co-transfected with expression vectors encoding V5-CARD14fl or V5-CARD14sh together with HA-BCL10 and FLAG-MALT1 vectors. MALT1 activity in cell lysates was then measured with a biotin-coupled activity based probe (ABP) that covalently modifies the active center of MALT1 (16). Immunoblotting of ABP streptavidin pulldowns indicated that the E138A variant of both V5-CARD14fl and V5-CARD14sh activated FLAG-MALT1, while activation of FLAG-MALT1 by WT versions of these proteins was very weak or absent (Figure 3A). Catalytically inactive C464A FLAG-MALT1 mutant was virtually undetectable in ABP pulldowns from lysates of cells co-expressing V5-CARD14fl^{E138A} or V5-CARD14sh^{E138A} and HA-BCL10, confirming the specificity of the MALT1 assay.

MALT1 protease activity can be inhibited by the phenothiazine mepazine by a non-competitive mechanism (23). To determine whether MALT1 paracaspase activity was required for CARD14 activation of NF-κB, HaCaT cells were transiently transfected with vectors encoding FLAG-CARD14sh^{E138A} or FLAG-CARD14fl^{E138A} and an NF-κB reporter and cultured in the presence of different concentrations of mepazine. NF-κB activation by both FLAG-CARD14sh^{E138A} and FLAG-CARD14fl^{E138A} was inhibited by mepazine, in a dose-dependent fashion (Figure 3B). Thus optimal stimulation of NF-κB by CARD14 was dependent on MALT1 paracaspase activity.

Maximal CARD14^{E138A}-induced gene expression depends on MALT1 paracaspase activity and MAP kinase signaling

Induction of B cell lymphoproliferation by an oncogenic CARD11 mutant is dependent on activation of both NF-κB and c-Jun N-terminal kinase (JNK) signaling cascades (24). To determine whether CARD14^{E138A} activated MAP kinase pathways in addition to NF-κB, HaCaT cells stably expressing Tet repressor (HaCaT-TR cells) (17) were transfected with FLAG-CARD14^{E138A} cDNA subcloned

into pcDNA5/TO and selected with hygromycin for 4-6 weeks (HaCaT-CARD14^{E138A} cells). Culture of the resulting cells with tetracycline rapidly induced the expression of FLAG-CARD14^{E138A} (Figure 4A). With similar kinetics, tetracycline treatment of HaCaT-CARD14^{E138A} cells stimulated IKK2 phosphorylation of NF-κB1 p105 (25). FLAG-CARD14^{E138A} expression also triggered activation loop phosphorylation of both ERK1/2 and p38α MAP kinases, while JNK activation loop phosphorylation was only weakly detectable after prolonged exposure. Culture of parental HaCaT-TRs cells with tetracycline did not induce phosphorylations of NF-κB1 p105, ERK1/2 or p38α ruling out any effects of tetracycline alone on signaling. Thus FLAG-CARD14^{E138A} stimulated the activation of ERK1/2 and p38α MAP kinase signaling pathways in keratinocytes, in addition to IKK2 / NF-κB.

We have previously shown that CARD14^{E138A} induces the expression in HEK001 keratinocytes of *IL8*, *CCL20* and *IL36γ* mRNAs (4), which are also elevated in psoriatic skin. The contribution of the IKK complex, MALT1 paracaspase activity and MAP kinase signaling to CARD14^{E138A}-induced expression of these genes was investigated in HaCaT-CARD14^{E138A} cells using pharmacological inhibitors and qRT-PCR. Treatment of cells with the IKK2 inhibitor BI605906 (26) essentially blocked expression of each of the genes following CARD14^{E138A} induction with tetracycline (Figure 4B). Inhibition of MALT1 paracaspase activity with mepazine (23) also substantially reduced FLAG-CARD14^{E138A}-induced *CCL20* mRNA expression and mildly impaired *IL8* induction, while not affecting *IL36γ* mRNA levels. Inhibition of ERK1/2 activation with the MEK1/2 inhibitor PD0325901 or p38α catalytic activity with VX-745 fractionally reduced *IL8* and *IL36γ* mRNA levels induced by FLAG-CARD14^{E138A}. These results indicate that CARD14^{E138A} principally promoted pro-inflammatory gene expression in keratinocytes via activation of IKK and NF-κB, while activation of ERK1/2 and p38α MAP kinase pathways was also required for maximal gene expression. In addition, MALT1 paracaspase activity was needed for optimal expression of specific targets genes by CARD14^{E138A}, reflecting the contribution of MALT1 activity to CARD14^{E138A} activation of NF-κB.

DISCUSSION

CARD14 is the causative gene within psoriasis susceptibility locus 2 (*PSORS2)* (3, 4). Dominant inherited gain-of-function mutations in CARD14 result in enhanced activation of NF-κB in keratinocytes, leading to psoriasis. In the current study, we demonstrated that *CARD14* psoriasis mutations induced the association of CARD14 with BCL10 and MALT1 to form a CARD14-BCL10-MALT1 complex that constitutively activated NF-κB. Each mutation abrogated an inhibitory effect of the linker region between the coiled-coil and PDZ domains, facilitating BCL10 binding to promote NF-κB activation. CARD14^{E138A} also activated the paracaspase activity of MALT1, which was required for optimal NF-κB activation and maximal expression of pro-inflammatory genes in keratinocytes.

The mechanism by which E138A and G117S mutations activate CARD14 signaling is analogous to that described for oncogenic CARD11 mutations in ABC DLBCL and other lymphomas (21). These disrupt an autoinhibitory interaction involving the CARD11 linker region (known as the Inhibitory Domain), resulting in constitutive formation of a CARD11-BCL10-MALT1 complex that activates NF-κB. However, activating CARD14 mutations in psoriasis are not linked to an increased incidence in skin cancer, which probably reflects differences in the physiology of keratinocytes compared to B cells. To mediate their function in adaptive immune responses, B cells must generate high affinity antibodies. Many of the genetic lesions that promote lymphomagenesis result from the aberrant activity of the RAG V(D)J recombinase and activation-induced cytidine deaminase (AID) enzymes that rearrange and mutate immunoglobulin genes in normal B cells (27). Oncogenic *CARD11* mutations cooperate with mutations in other genes to transform B cells, including *MyD88*, *BCL6* and *PRDM1* (21). It is possible that the lack of RAG and AID enzymes in keratinocytes make generation of secondary activating mutations to cooperate with mutant CARD14 significantly less likely.

Although there are similarities between the effects of oncogenic CARD11 mutations and psoriasis mutations in CARD14, the downstream consequences are not identical. A recent study has shown that the L225LI gain-of-function CARD11 mutant activates JNK and NF-κB to promote B cell proliferation (24). In contrast, CARD14^{E138A} expression in keratinocytes activated NF-κB, ERK1/2 and p38α, but activation of JNK was barely detectable. Furthermore, although NF-κB activation was an absolute requirement of the expression of *IL8*, *CCL20* and *IL36γ* downstream of CARD14^{E138A}, activation of ERK1/2 and p38α was required for

maximal induction of *IL8* and *IL36γ*. Interestingly, increased levels of activated ERK1/2 and p38α are detected in lesional psoriatic skin compared to non-lesional skin, while JNK activation is not altered (28). These results suggest that CARD11 and CARD14 are wired differently to downstream effectors. MALT1 inhibition by mepazine also exerted differential effects on the induction of CARD14^{E138A} induced genes leading to reduced *CCL20* and *IL8* induction while *IL36 γ* was unaffected. It is possible that we did not observe stronger effects of MALT1 inhibition as NF-κB activation was only partially inhibited by mepazine. This was demonstrated in our transient transfection system where mepazine-mediated inhibition of CARD14sh/fl^{E138A}-induced NF-κB reporter activity was only partial. Thus, residual NF-κB activity may have been sufficient to fully induce *IL36γ* expression. Alternatively, as two critical posttranscriptional regulators, Regnase-1 and Roquin1/2, were recently identified as MALT1 substrates (29, 30), it is possible that MALT1-dependent regulation of mRNA stability could also contribute to the differential effects on distinct on gene expression. It will be important in future studies to elucidate the components of the signaling pathways that link CARD14 to the downstream activation of NF-κB, MALT1, ERK1/2 and p38α in keratinocytes. In order to understand the normal regulation of CARD14, it will also be necessary to determine whether wild type CARD14 activation involves phosphorylation of the inhibitory linker domain by PKC isoforms like CARD11 and to identify physiological upstream activating receptors.

Psoriasis is usually considered to be a multi-factorial disease (2) and current models of psoriasis pathogenesis propose a complex interplay between activated keratinocytes and immune cells, with a key role for T lymphocytes (1). As CARD14 expression is largely restricted to keratinocytes and endothelial cells (4, 14), it is likely that gain-of-function *CARD14* mutations promote psoriasis by generating an environment of chronic pro-inflammatory signaling and cytokine/chemokine expression in the skin. This will lead to the recruitment of immune cells including T cells producing IL-17 and IL-22 cytokines, which enhance keratinocyte activation and sustain skin inflammation (1). However, whether gain-of-function CARD14 mutations are sufficient for the initiation (as opposed maintenance) of psoriatic disease is currently unclear. CARD14^{E138A} and CARD14^{G117S} activate NF-κB when expressed in keratinocytes *in vitro* (this study and (4)). However, the age of onset of psoriatic disease in patients harboring these mutations is variable (3, 4). Thus additional factors may contribute to psoriasis pathogenesis in individuals harboring CARD14 mutations, which may be environmental triggers or possibly epigenetic alterations. The fact that CARD14

pathogenic alterations are highly penetrant suggests that additional genetic factors are unlikely to be required, although they could contribute to disease severity or onset of PsA. Consistent with this hypothesis, it has recently been proposed that the onset of CARD14^{G117S} associated psoriatic disease may be earlier in the presence of the psoriasis-risk allele *HLA-C*06:02* (31).

Currently, anti-TNF biologics are one of the most effective treatments for both psoriasis and psoriatic arthritis (NICE guidelines [CG153], 2012). However, anti-TNF therapies are expensive, require injection and can impair the immune response to pathogens. In addition, a fraction of patients do not respond to anti-TNF, or their response diminishes over time (32). Furthermore, patients have been described in which psoriatic lesions are exacerbated following anti-TNF therapy (33). The new biologic ustekinaumab (which binds the p40 subunit of IL-12 and IL-23) ameliorates psoriasis in the majority of patients (34). However, anti-p40 is less effective for PsA, and in a subset of patients arthritic symptoms worsen with anti-p40 therapy (35). Similarly, while anti-IL-17 is very effective in treatment of psoriasis (36), its effects on PsA are more modest (37). Our study has demonstrated that MALT1 paracaspase activity is required for activation of NF-κB and induced expression of key pro-inflammatory genes by rare gain-of-function CARD14 variants. The common R820W variant of CARD14 predisposes individuals to psoriasis in European and Chinese populations (3, 12), placing CARD14 in the pathway to common psoriasis. This raises the interesting possibility that MALT1 inhibitors might have beneficial effects for treatment of psoriasis and PsA.

ACKNOWLEDGEMENTS

The authors would like to thank Caroline Hill for providing the HaCaT-TR cell line.

AUTHOR CONTRIBUTION

AH co-designed the study, performed the majority of the experiments, and co-wrote the manuscript. POS, FB and AG performed some experiments. LC performed preliminary experiments on the project. DK advised on methodology and experimental design, and critically reviewed the manuscript. AMB co-supervised the study and critically reviewed the manuscript. SCL co-designed, co-supervised, and co-wrote the manuscript.

CONFLICT OF INTEREST

The authors declare that they have no conflict of interest.

FUNDING

This research was supported by grant AR050266 from the National Institutes of Health (USA) (A.M.B.), a grant of the Wilhelm-Sander Stiftung (GER) (DK) and core funding from The Francis Crick Institute (UK) (SCL).

REFERENCES

1. Lowes M. A., Suarez-Farinas M., Krueger J. G. (2014) Immunology of psoriasis. Ann Rev Immunol. **32**, 227 - 55.
2. Harden J. L., Krueger J. G., Bowcock A. M. (2015) The immunogenetics of psoriasis: a comprehensive review. J Autoimmun. **64**, 66 - 73.
3. Jordan C. T., Cao L., Roberson E. D., Duan S., Helms C. A., Nair R. P., Duffin K. C., Stuart P. E., Goldgar D., Hayashi G., Olfson E. H., Feng B.-J., Pullinger C. R., Kane J. P., Wise C. A., Goldback-Mansky R., Lowes M. A., Peddle L., Chandran V., Liao W., Rahman P., Krueger G. G., Gladman D., Elder J. T., Menter A., Bowcock A. M. (2012) Rare and common variants in CARD14, encoding an epidermal regulator of NF-κB, in psoriasis. Am J Hum Genet. **90**, 796 - 808.
4. Jordan C. T., Cao L., Roberson E. D., Pierson K. C., Yang C. F., Joyse C. E., Ryan C., Duan S., Helms C. A., Liu Y., Chen Y., A. M. A., Hwu W. L., Wu J. Y., Chen Y. T., Menter A., Goldbach-Mansky R., Lowes M. A., Bowcock A. M. (2012) PSORS2 is due to mutations in CARD14. Am J Hum Genet. **90**, 784 - 95.
5. Ammar M., Jordan C. T., Cao L., Lim E., Bouchlaka Souissi C., Jrad A., Omrane I., Kouidhi S., Zaraa I., Anbunathan H., Mokni M., Doss N., Guttman-Yassky E., El Gaaied A. B., Menter A., Bowcock A. M. (2016) CARD14 alterations in Tunisian patients with psoriasis and further characterization in European cohorts. Br J Dermatol. **174**, 330 - 7.
6. Tsoi L. C., Spain S. L., Knight J., Ellinghaus E., Stuart P. E., Capon F., Ding J., Li Y., Tejasvi T. (2012) Identification of 15 new psoriasis susceptibility loci highlights the role of innate immunity. Nat Genetics. **44**, 1341 - 8.
7. Cheng H., Li Y., Zuo X. B., Tang H. Y., Tang X. F., Gao J. P., Sheng Y. J., Yin X. Y., Zhou F. S., Zhang C., Chen G., Zhu J., Pan Q., Liang B., Zheng X. D., Li P., Ding Y. T., Cheng F., Luo J., Chang R. X., Pan G. B., Fan X., Wang Z. X., Zhang A. P., Liu J. J., Yang S., Sun L. D., Zhang X. J. (2014) Identification of a missense variant in LNPEP that confers psoriasis risk. J Invest Dermatol. **134**, 359 - 65.
8. Bowes J., Budu-Aggrey A., Huffmeier U., Uebe S., Steel K., Hebert H. L., Wallace C., Massey J., Bruce I. N., Bluett J., Feletar M., Morgan A. W., Marzo-Ortega H., Donohoe G., Morris D. W., Helliwell P., Ryan A. W., Kane D., Warren R. B., Korendowych E., Alenius G. M., Giardina E., Packham J., McManus R., Fitzgerald O., McHugh N., Brown M. A., Ho P., Behrens F., Burkhardt H., Reis A., Barton A. (2015) Dense genotyping of immune-related susceptibility loci reveals new insights into the genetics of psoriatic arthritis. Nat Commun. **6**, 6046.
9. Jiang C., Lin X. (2012) Regulation of NF-κB by the CARD proteins. Immunol Rev. **246**, 141 - 53.
10. Ghosh S., May M. J., Kopp E. B. (1998) NF-kB and Rel proteins: evolutionary conserved mediators of immune responses. Annu Rev Immunol. **16**, 225-60.
11. Bertin J., Wang L., Guo Y., Jacobson M. D., Poyet J.-L., Srinivasula S. M., Merriam S., DiStefano P. S., Alnemri E. S. (2001) CARD11 and CARD14 are novel caspase recruitment domain (CARD) / membrane-associated guanylate kinase (MAGUK) family members that interact with BCL10 and activate NF-κB. J Biol Chem. **276**, 11877 -82.
12. Scudiero I., Zotti T., Ferravante A., Vessichelli M., Vito P., Stilo R. (2011) Alternative splicing of CARMA2/CARD14 transcripts generates protein variants with differential effect on NF-κB activation and endoplasmic reticulum stress-induced cell death. J Cell Pysiol. **226**, 3121 - 31.
13. Goldminz A. M., Au S. C., Kim N., Gottlieb A. B., Lizzul P. F. (2013) NF-kB: an essential transcription factor in psoriasis. J Derm Sci. **69**, 89 - 94.

14. Harden J. L., Lewis S. M., Pierson K. C., Suarez-Farinas M., Lentini T., Ortenzio F. S., Zaba L. C., Goldbach-Mansky R., Bowcock A. M., Lowes M. A. (2014) CARD14 expression in dermal endothelial cells in psoriasis. PLOS One. **9**, e111255.
15. Afonina I. S., Elton L., Carpentier I., Beyaert R. (2015) MALT1 - a universal soldier: multiple strategies to ensure NF-kB activation and target gene expression. FEBS J. **282**, 3286 - 97.
16. Eitelhuber A. C., Vosyka O., Nagel D., Bognar M., Lenze D., Lammens K., Schlauderer F., Hlahla D., Hopfner K.-P., Lenz G., Hummel M., Verhelst S. H. L., Krappmann D. (2015) Activity-based probes for detection of active MALT1 paracaspase in immune cells and lymphomas. Chem Biol. **22**, 139 - 47.
17. Levy L., Hill C. S. (2005) Smad4 dependency defines two classes of transforming growth factor beta (TGFb) target genes and distinguishes TGFb-induced epithelial-mesenchymal transition from its antiproliferative and migratory responses. Mol Cell Biol. **25**, 8108 - 25.
18. Jiang C., Lin X. (2012) Regulation of NF-kappaB by the CARD proteins. Immunological reviews. **246**(1), 141-53.
19. McCully R. R., Pomerantz J. L. (2008) The protein kinase C-responsive inhibitory domain of CARD11 functions in NF-kB activation to regulate the association of multiple signaling cofactors that differentially depend on Bcl10 and MALT1 for association. Mol Cell Biol. **28**, 5668 - 86.
20. Sommer K., Guo B., Pomerantz J. L., Bandaranayake A. D., Moreno-Garcia M. E., Ovechkina Y. L., Rawlings D. J. (2005) Phosphorylation of the CARMA1 linker controls NF-kB activation. Immunity. **23**, 561 - 74.
21. Lamason R. L., McCully R. R., Lew S. M., Pomerantz J. L. (2010) Oncogenic CARD11 mutations induce hyperactive signaling by disrupting autoinhibition by the PKC-responsive inhibitory domain. Biochem. **49**, 8240 - 50.
22. Lim K.-H., Yang Y., Staudt L. M. (2012) Pathogenetic importance and therapeutic implications of NF-kB in lymphoid malignancies. Immunol Rev. **246**, 359 - 78.
23. Nagel D., Spranger S., Vincendeau M., Grau M., Raffegerst S., Kloo B., Hlahla D., Neuenschwander M., von Kries J. P., Hadian K., Dorken B., Lenz P., Lenz G., Schendel D. J., Krappmann D. (2012) Pharmacologic inhibition of MALT1 protease by phenothiazines as a therapeutic approach for the treatment of aggressive ABC-DLBCL. Cancer Cell. **22**, 825 - 37.
24. Knies N., Alankus B., Weilemann A., Tzankov A., Brunner K., Ruff T., Kremer M., Keller U. B., Lenz G., Ruland J. (2015) Lymphomagenic CARD11/BCL10/MALT1 signaling drives malignant B-cell proliferation via cooperative NF-kB and JNK activation. Proc Natl Acad Sci USA. **112**, E7230 - 8.
25. Lang V., Janzen J., Fischer G. Z., Soneji Y., Beinke S., Salmeron A., Allen H., Hay R. T., Ben-Neriah Y., Ley S. C. (2003) bTrCP-mediated proteolysis of NF-kB1 p105 requires phosphorylation of p105 serines 927 and 932. Mol Cell Biol. **23**, 402-13.
26. Clark K., Peggie M., Plater L., Sorcek R. J., Young E. R. R., Madwed J. B., Hough J., McIver E. G., Cohen P. (2011) Novel cross-talk within the IKK family controls innate immunity. Biochem J. **434**, 93 - 104.
27. Robbiani D. F., Nussenzweig M. C. (2012) Chromosome translocation, B cell lymphoma, and activation-induced cytidine deaminase. Ann REv Pathol Mech Dis. **8**, 79 - 103.
28. Johansen C., Kragballe K., WEstergaard M., Henningsen J., Kristiansen K., Iverson L. (2005) The mitogen-activated protein kinase p38 and ERK1/2 are increased in lesional psoriatic skin. Br J Dermatol. **152**, 37 - 42.
29. Uehata T., Iwasaki H., Vandenbron A., Matsushita K., Hernandez-Cuellar E., Kuniyoshi K., Satoh T., Mino T., Suzuki Y., Standley D. M., Tsujimura

T., Rakugi H., Isaka Y., Takeuchi O., Akira S. (2013) Malt1-induced cleavage of regnase-1 in CD4+ helper T cells regulates immune activation. Cell. **153**, 1036 - 49.

30. Jeltsch K. M., Hu D., Brenner S., Zöller J., Heinz G. A., Nagel D., Vogel K. U., Rehage N., Warth S. C., Edelmann S. L., Gloury R., Martin N., Lohs C., Lech M., Stehklein J. E., Geerlof A., Kremmer E., Weber A., Anders H. J., Schmitz I., Schmidt-Supprian M., Fu M., Holtmann H., Krappmann D., Ruland J., Kallies A., Heikenwalder M., Heissmeyer V. (2014) Cleavage of roquin and regnase-1 by the paracaspase MALT1 releases their cooperatively repressed targets to promote Th17 differentiation. Nat Immunol. **15**, 1079 - 89.
31. Eskin-Schwartz M., Basel-Vanagaite L., David M., Lagovsky I., Ben-Amitai D., Smirin-Yosef P., Atzmony L., Hodak E. (2016) Intra-familial Variation in Clinical Phenotype of CARD14-related Psoriasis. Acta dermato-venereologica.
32. Leman J., Burden A. D. (2012) Sequential use of biologics in the treatment of moderate-to-severe plaque psoriasis. Br J Dermatol. **167**, 12 - 20.
33. Callamer A. N., Guerrero K. T., Henning J. S., Battafarano D. F. (2008) Psoriatic skin lesions induced by tumor necrosis factor antagonist therapy: a literature review and potential mechanisms of action. Arthritis Rheum. **59**, 996 - 1001.
34. Olivieri I., D'Angelo S., Palazzi C., Padula A. (2014) Advances in the management of psoriatic arthritis. Nat Rev Rheumatol. **10**, 531 - 42.
35. de Souza A., Ali-Shaw T., Reddy S. M., Fiorentino D., Strober B. E. (2013) Inflammatory arthritis following ustekinumab treatment for psoriasis: a report of two cases. Br J Dermatol. **168**, 210 - 2.
36. Belge K., Brück J., Ghoreschi K. (2014) Advances in treating psoriasis. F1000 Prime Reports. **6**, 4.
37. McInnes I. B., Sieper J., Braun J., Emery P., van der Heijde D., Isaacs J. D., Dahmen G., Wollenhaupt J., Schulze-Koops H., Kogan J., Ma S., Schumacher M. M., Bertolino A. P., Hueber W., Tak P. P. (2014) Efficacy and safety of secukinumab, a fully human anti-interleukin-17A monoclonal antibody, in patients with moderate-to-severe psoriatic arthritis: a 24-week, randomised, double-blind, placebo-controlled, phase II proof-of-concept trial. Ann Rheum Dis. **73**, 349 - 56.

Figure 1. Psoriasis associated CARD14 mutants require BCL10 and MALT1 to activate NF-κB.

(**A**) Schematic of CARD14 domains and psoriasis-associated mutations. (**B, C**) HEK293 cells were co-transfected with vectors encoding the indicated V5-CARD14 variants (0.1-1.2 μg), FLAG-MALT1 (1 μg) and HA-BCL10 (0.6-1.2 μg). Anti-FLAG immunoprecipitates were immunoblotted with the indicated antibodies. Representative of at least two independent experiments. (**D, E**) HaCaT keratinocytes were co-transfected with vectors encoding the indicated FLAG-CARD14 variants (0.125-0.2 μg) or empty vector (EV), pNFκB-Luc and pRL-TK. After 24 h, NF-κB activity was determined by luciferase assay (mean ± SEM of three independent experiments). FLAG-CARD14 expression was determined by immunoblotting of lysates. Significance determined by t-test. (**F, G**) HaCaT keratinocytes were transfected with *Bcl10* or *Malt1* siRNA pools or control non-targeting pool. After 48 h, cells were transfected with FLAG-CARD14 variants (0.05-0.1 μg), pNFκB-Luc and pRL-TK vectors and cultured for a further 24 h. NF-κB activity was determined as in D (mean ± SEM of three independent experiments). Representative expression of FLAG-CARD14, endogenous BCL10 and endogenous MALT1 was determined by immunoblotting of corresponding lysates. Significance determined by two-way ANOVA.

Figure 2. Abrogation of CARD14 inhibitory linker region activity by deletion or psoriasis mutation induces BCL10 association.

(**A, B**) HaCaT keratinocytes were co-transfected with FLAG-CARD14 (0.125-0.2 μg), pNFκB-Luc and pRL-TK plasmids. NF-κB activity was determined as in Figure 1D (mean ± SEM of three independent experiments). Representative expression of FLAG-CARD14 and tubulin in corresponding lysates was determined by immunoblotting. Significance determined by two-way ANOVA. LR; linker region, FC; fold change. (**C**) Fold change (FC) NF-κB activation of mutant *versus* WT CARD14, in the presence or absence of the LR (calculated from data in figures 2 A and B). Mean ± SEM of three independent experiments. Significance determined by t-test. (**D**) HEK293 cells were co-transfected with vectors encoding the indicated V5-CARD14 variants (0.1-1 μg) and FLAG-BCL10 (0.6-0.8 μg). Anti-FLAG immunoprecipitates were immunoblotted with the indicated antibodies. Representative of three independent experiments.

Figure 3. CARD14^{E138A} mutation activates MALT1 paracaspase activity.
(**A**) HEK293 cells were co-transfected with vectors encoding V5-CARD14 variants (0.1-0.4 μg), WT or C464 FLAG-MALT1 (0.8-1.2 μg) and HA-BCL10 (0.8-1.4 μg). Active MALT1 was assayed by activity based probe (ABP) pull down and immunoblotting. Representative of three independent experiments. (**B**) HaCaT keratinocytes were co-transfected with FLAG-CARD14 variant (0.125-0.2 μg) or EV, pNFκB-Luc and pRL-TK vectors. 5 h after transfection, cells were treated with mepazine or DMSO vehicle and lysed after further 24 h culture. NF-κB activity was determined as in Figure 1D (mean ± SEM of three independent experiments). Representative expression of FLAG-CARD14 was determined by immunoblotting of corresponding lysates. Significance determined by two-way ANOVA.

Figure 4. CARD14^{E138A}-induced gene expression is dependent on IKK2, MALT1, ERK1/2 and p38α activity.
(**A**) HaCaT-TR or HaCaT-CARD14^{E138A} cells were treated with tetracycline for the indicated times. CARD14^{E138A} expression and phosphorylation of indicated proteins was determined by immunoblotting. Representative of three independent experiments using two independently generated stable cultures. (**B - D**) HaCaT-CARD14^{E138A} cells were pre-treated with BI605906 (10 μM, IKK2 inhibitor), mepazine (MALT1 inhibitor), PD0325901 (0.1 μM, MEK1/2 inhibitor), VX-745 (1 μM, p38α inhibitor) or DMSO vehicle for 1 h, and cultured for a further 6 h after subsequent tetracycline addition. Gene expression was assayed by qRT-PCR (mean ± SD, n=3). Significance determined by two-way ANOVA. Representative of at least two independent experiments using independently generated stable cultures.

Figure 1

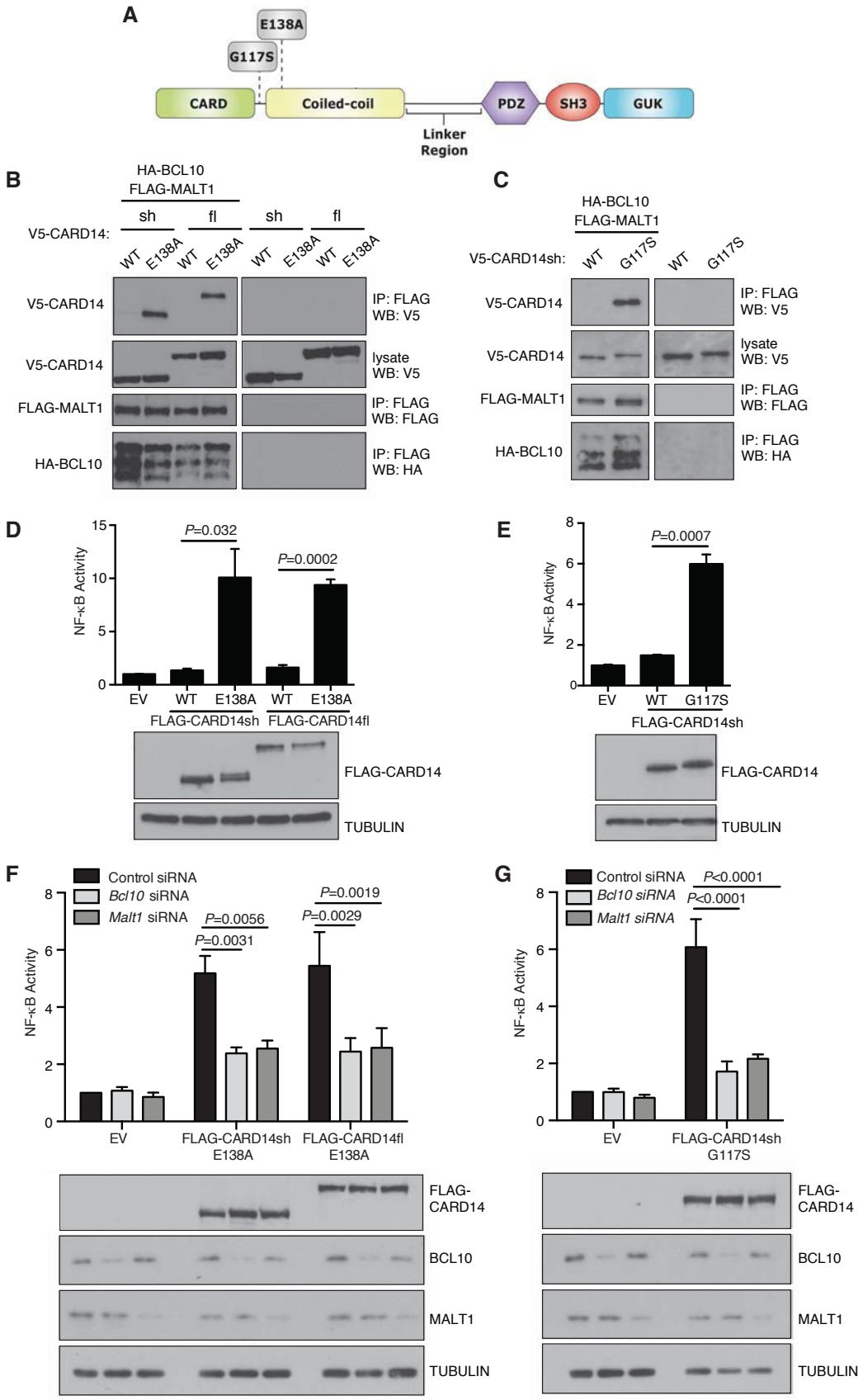
A
E138A
G117S
CARD
Coiled-coil
PDZ
SH3
GUK
Linker Region
B
HA-BCL10
FLAG-MALT1
sh
fl
V5-CARD14:
WT
E138A
V5-CARD14
FLAG-MALT1
HA-BCL10
IP: FLAG WB: V5
lysate WB: V5
IP: FLAG WB: FLAG
IP: FLAG WB: HA
C
V5-CARD14sh:
G117S
D
NF-κB Activity
P=0.032
P=0.0002
EV
FLAG-CARD14sh
FLAG-CARD14fl
FLAG-CARD14
TUBULIN
E
P=0.0007
G117S
F
Control siRNA
Bcl10 siRNA
Malt1 siRNA
P=0.0056
P=0.0031
P=0.0019
P=0.0029
FLAG-CARD14sh E138A
FLAG-CARD14fl E138A
BCL10
MALT1
G
P<0.0001
FLAG-CARD14sh G117S

Figure 2

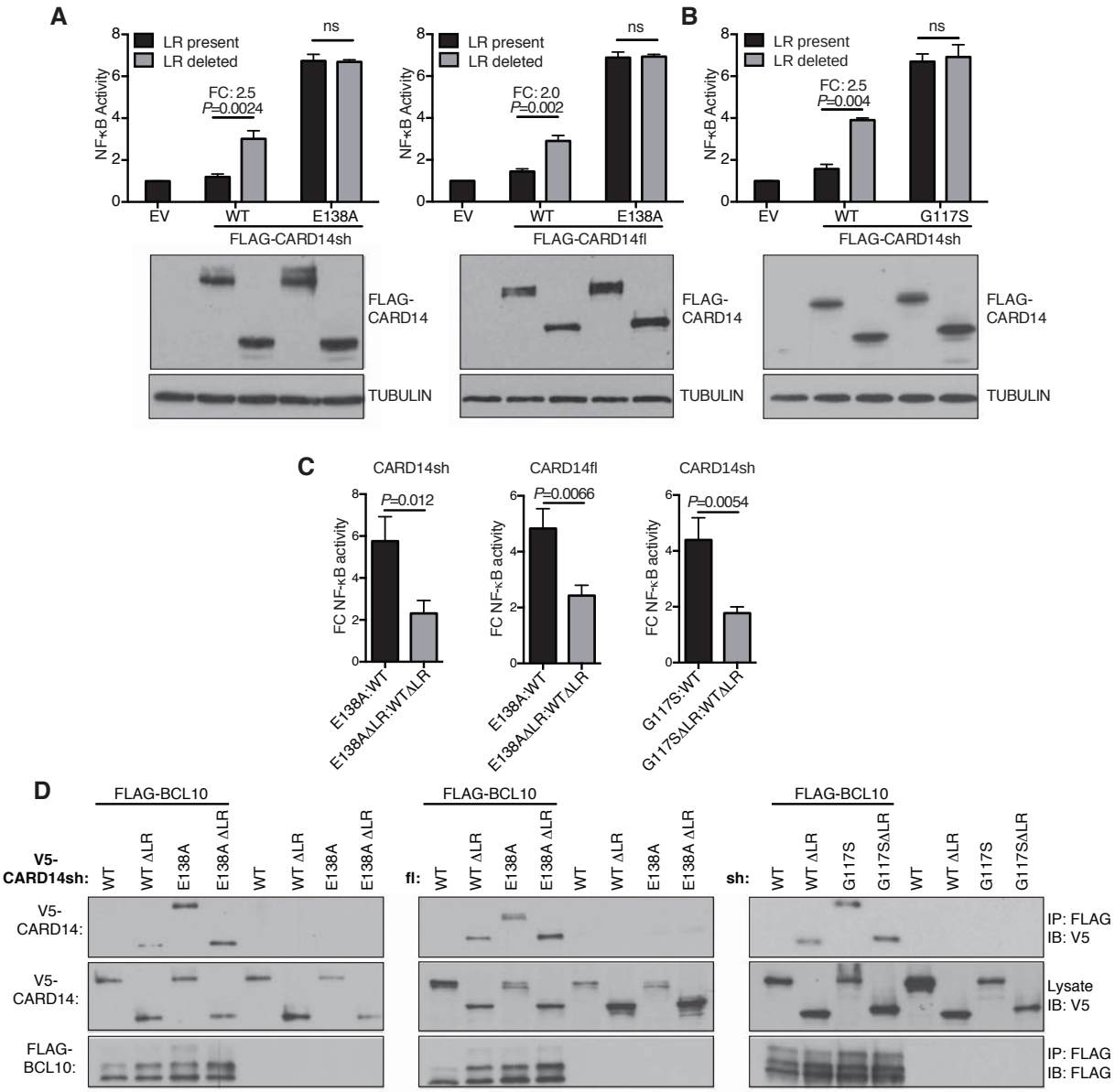
A
LR present
LR deleted
NF-κB Activity
FC: 2.5
P=0.0024
ns
EV
WT
E138A
FLAG-CARD14sh
FC: 2.0
P=0.002
FLAG-CARD14fl
B
FC: 2.5
P=0.004
G117S
FLAG-CARD14sh
FLAG-CARD14
TUBULIN
C
CARD14sh
CARD14fl
CARD14sh
FC NF-κB activity
P=0.012
P=0.0066
P=0.0054
E138A:WT
E138AΔLR:WTΔLR
G117S:WT
G117SΔLR:WTΔLR
D
FLAG-BCL10
V5-CARD14sh:
WT
WT ΔLR
E138A
E138A ΔLR
fl:
G117S
G117SΔLR
sh:
V5-CARD14:
FLAG-BCL10:
IP: FLAG
IB: V5
Lysate
IB: V5
IP: FLAG
IB: FLAG

Figure 3

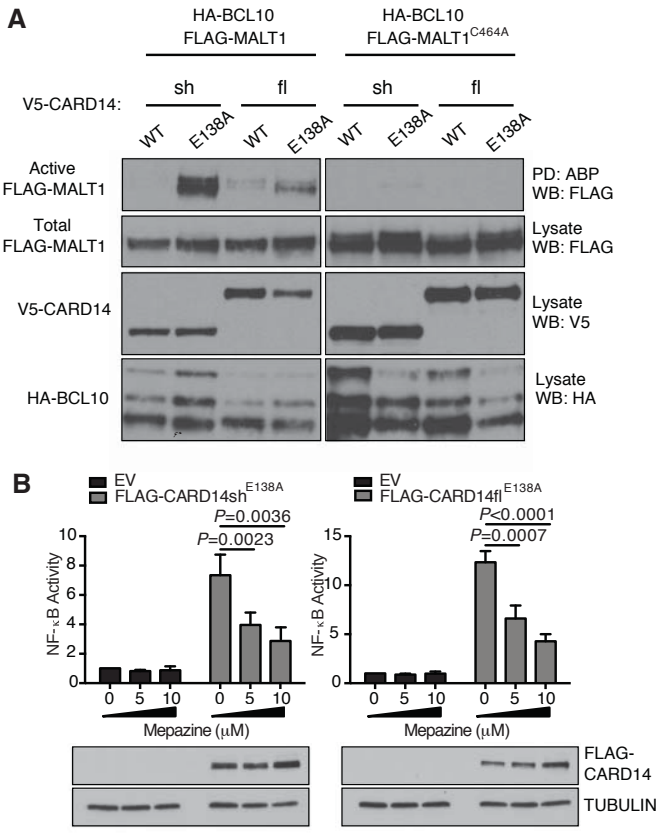
A
HA-BCL10
FLAG-MALT1
HA-BCL10
FLAG-MALT1C464A
V5-CARD14:
sh
fl
sh
fl
WT
E138A
WT
E138A
WT
E138A
WT
E138A
Active FLAG-MALT1
PD: ABP
WB: FLAG
Total FLAG-MALT1
Lysate
WB: FLAG
V5-CARD14
Lysate
WB: V5
HA-BCL10
Lysate
WB: HA
B
EV
FLAG-CARD14shE138A
P=0.0036
P=0.0023
NF-κB Activity
0
2
4
6
8
10
0 5 10 0 5 10
Mepazine (μM)
EV
FLAG-CARD14flE138A
P<0.0001
P=0.0007
NF-κB Activity
0
5
10
15
0 5 10 0 5 10
Mepazine (μM)
FLAG-CARD14
TUBULIN

Figure 4

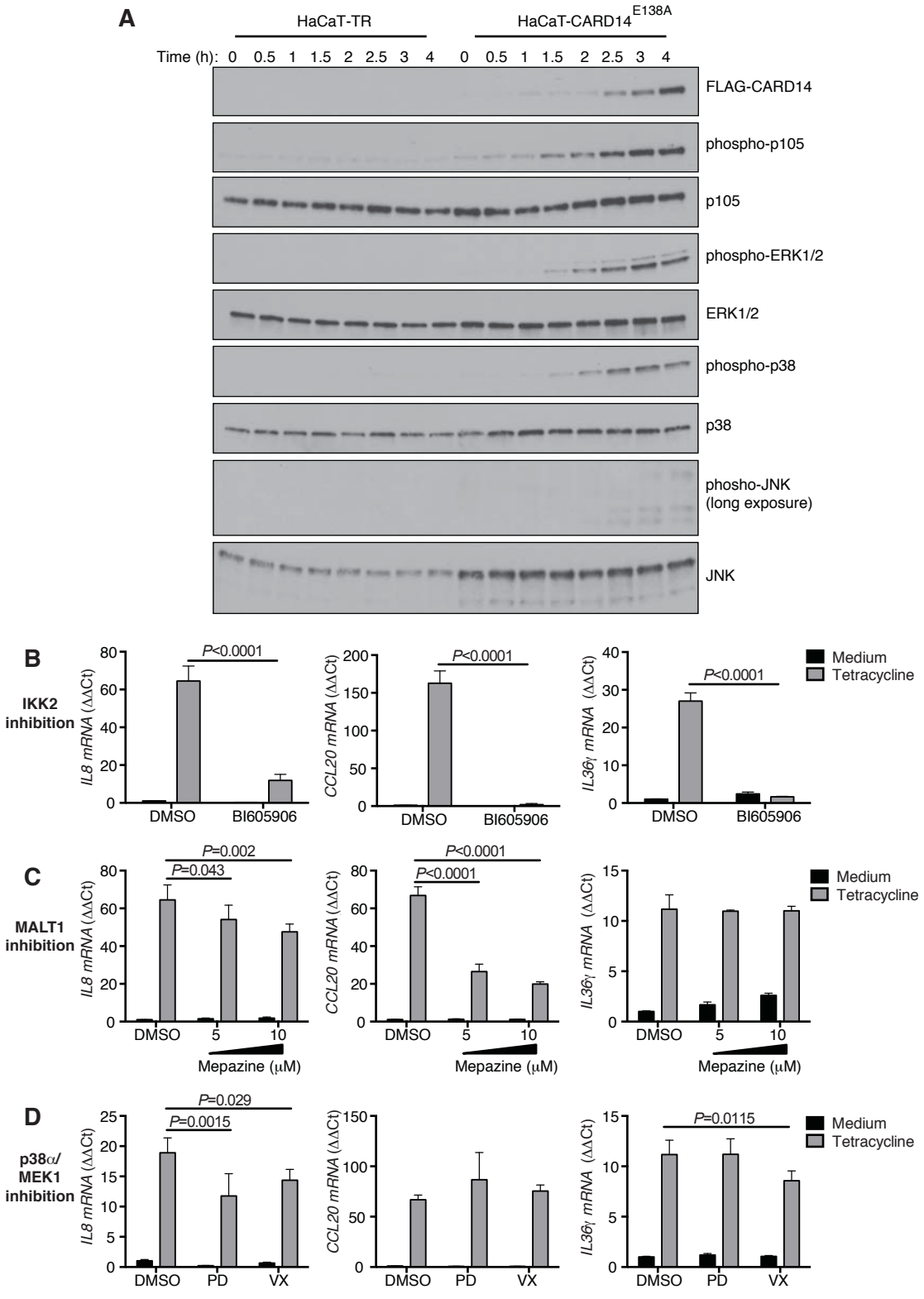
A
HaCaT-TR
HaCaT-CARD14 E138A
Time (h): 0 0.5 1 1.5 2 2.5 3 4 0 0.5 1 1.5 2 2.5 3 4
FLAG-CARD14
phospho-p105
p105
phospho-ERK1/2
ERK1/2
phospho-p38
p38
phosho-JNK (long exposure)
JNK
B
IKK2 inhibition
IL8 mRNA (ΔΔCt)
CCL20 mRNA (ΔΔCt)
IL36γ mRNA (ΔΔCt)
P<0.0001
DMSO
BI605906
Medium
Tetracycline
C
MALT1 inhibition
P=0.002
P=0.043
P<0.0001
Mepazine (μM)
D
p38α/ MEK1 inhibition
P=0.029
P=0.0015
P=0.0115
PD
VX